ResearchGate

See discussions, stats, and author profiles for this publication at: https://www.researchgate.net/publication/251567810

Disentangling Electronic and Vibronic Coherences in Two-Dimensional Echo Spectra

ARTICLE *in* THE JOURNAL OF PHYSICAL CHEMISTRY B · JULY 2013

Impact Factor: 3.3 · DOI: 10.1021/jp405421d · Source: PubMed

CITATIONS
24

READS
36

3 AUTHORS, INCLUDING:

Christoph Kreisbeck
Harvard University
20 PUBLICATIONS **267** CITATIONS
SEE PROFILE

Alán Aspuru-Guzik
Harvard University
249 PUBLICATIONS **5,076** CITATIONS
SEE PROFILE

Available from: Alán Aspuru-Guzik
Retrieved on: 27 January 2016

THE JOURNAL OF PHYSICAL CHEMISTRY B

Article

pubs.acs.org/JPCB

Disentangling Electronic and Vibronic Coherences in Two-Dimensional Echo Spectra

Christoph Kreisbeck,[†] Tobias Kramer,*[,‡,§] and Alán Aspuru-Guzik[†]

[†]Department of Chemistry and Chemical Biology, Harvard University, 12 Oxford Street, Cambridge, Massachusetts 02138, United States

[‡]Institut für Physik, Humboldt Universität zu Berlin, Newtonstr. 15, 12489 Berlin, Germany

[§]Department of Physics, Harvard University, 17 Oxford Street, Cambridge, Massachusetts 02138, United States

ABSTRACT: The prevalence of long-lasting oscillatory signals in two-dimensional (2D) echo spectroscopy of light-harvesting complexes has led to a search for possible mechanisms. We investigate how two causes of oscillatory signals are intertwined: (i) electronic coherences supporting delocalized wavelike motion and (ii) narrow bands in the vibronic spectral density. To disentangle the vibronic and electronic contributions, we introduce a time-windowed Fourier transform of the signal amplitude. We find that 2D spectra can be dominated by excitations of pathways which are absent in excitonic energy transport. This leads to an underestimation of the lifetime of electronic coherences by 2D spectra.

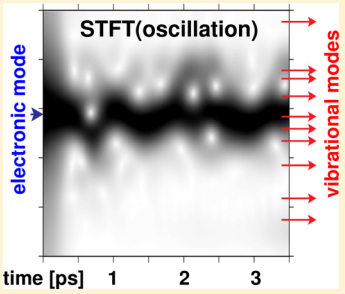

INTRODUCTION

The observation of long-lasting oscillations in peak amplitudes of two-dimensional (2D) echo spectroscopy as a function of increasing delay time between pump and probe pulses[1−6] has led to an intensive search for quantum mechanical effects in photosynthetic systems at physiological temperatures. The general theoretical model of excitonic energy transfer from the antenna to the reaction center is well-established.[7−9] For the Fenna−Matthews−Olson (FMO) complex, an efficient transfer relies on a dissipative coupling of electronic and vibronic degrees of freedom,[10−16] which puts the excited system in an energy funnel toward the reaction center. The oscillations recorded in 2D echo spectra were not anticipated within a simplified rate equation formalism based on Markovian approximations for the dissipative coupling of vibronic and electronic degrees of freedom.[17,18]

The physical origin of the experimental observations has led to various theoretical proposals, which are roughly divided into two mechanisms. As shown from calculations in model Hamiltonians,[19−22] the presence of δ-spiked peaks in the vibronic mode distribution does imprint a long-lasting oscillatory signal on coherences. The spectral density determined from fluorescence line-narrowing experiments (J_{Wendling} in Figure 1) reveals a series of peaks. However, a calculation of 2D spectra and coherences[25] using a close approximation to the density (denoted by $J_{3\mathrm{peaks}}$ and $J_{11\mathrm{peaks}}$ in Figure 1) puts the vibronic contributions on a scale much smaller than that of electronic coherences, which lead to oscillation periods determined by the differences in excitonic eigenenergies. The second proposed mechanism[25] identifies two prerequisites for long-lasting electronic coherences and oscillations of cross-peaks of 2D spectra in the continuous part of the vibronic mode distribution: (i) a small initial slope of the vibronic density toward zero frequency and (ii) a larger coupling between a continuum of vibrations whose frequencies are in the range of the typical excitonic energy gaps. Both conditions are fullfilled by the florescence line-narrowing spectral density J_{Wendling}.

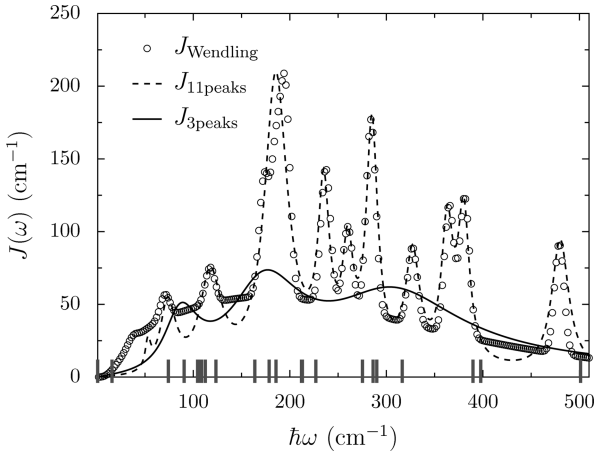

Figure 1. Spectral density of the FMO complex. Circles: measured spectral density[23] and parametrization.[24] Fits $J_{\{3,11\}\mathrm{peaks}}$ are used for the GPU−HEOM calculation. The marks on the frequency axis indicate differences of exciton eigenenergies.

It remains an open question to what extent 2D spectra are probing vibrational or electronic properties of light-harvesting complexes. The experimental data show oscillations of cross-peaks lasting about 1 ps at T = 150 K,[5] which exceed the

Received: June 1, 2013
Revised: July 19, 2013
Published: July 23, 2013

 © 2013 American Chemical Society dx.doi.org/10.1021/jp405421d | J. Phys. Chem. B 2013, 117, 9380−9385

theoretical values by a factor of 2 based on the calculations of 2D spectra within the Frenkel exciton model.[25] To provide a more comprehensive picture based on atomistic approaches, theoretical models beyond the Frenkel exciton approach in combination with studies of the vibrational mode distribution are required.[26−28] Moreover, for the design of artificial nanostructures it is of interest to identify the physical mechanism of efficient transport and conditions for the accompanying vibronic density. Here, we disentangle the interplay of electronic and vibronic effects on the transport by introducing a reliable method to dissect the 2D echo signal. We show that a time-windowed short-time Fourier transform (STFT) is a suitable tool to track and assign specific vibronic and electronic contributions at all delay times. We find that two-dimensional echo spectra can significantly *underestimate* the duration of electronic coherences because of the destructive superposition of several pathways related to additional excitations and ground-state bleaching. Such pathways are not important for excitonic energy transfer, which for the same system displays longer electronic coherences than the 2D spectra. The connection between 2D spectra and efficient transport and the role of coherences require careful evaluation.

TRANSITION FROM ELECTRONIC TO VIBRATIONAL INDUCED COHERENCE IN THE FMO COMPLEX

Multiple frequencies are a common pattern in the cross-peak oscillations observed in 2D echo spectra of various light-harvesting complexes such as the FMO complex[29,30] or light-harvesting proteins PE545 and PC645 from marine cryptophyte algae.[3,6] To unravel which physical processes are present as the delay time progresses and to uncover the transition from electronic to vibrational induced coherences, we introduce a windowed STFT of the signal

$$\mathcal{F}_{\mathrm{w}}(\omega, t_{\mathrm{c}})\, \rho_{E_iE_k}(t) = \int_{-\infty}^{\infty} \mathrm{d}t\, F_{\mathrm{w}}(t_{\mathrm{c}}, t)\, \rho_{E_iE_k}(t)\, e^{\mathrm{i}\omega t} \tag{1}$$

where t_{c} denotes the center and t_{w} the width of the window function

$$F_{\mathrm{w}}(t_{\mathrm{c}}, t) = \sum_{s=\pm 1} \frac{s}{1 + \exp[\beta(t - t_{\mathrm{c}} - s t_{\mathrm{w}}/2)/t_{\mathrm{w}}]} \tag{2}$$

Later, we normalize $\mathcal{F}_{\mathrm{w}}(t_{\mathrm{c}})\rho_{E_iE_k}$ to its maximal value. A typical window function with the calculated coherence between exciton eigenstates $|E_1\rangle$ and $|E_S\rangle$ of the FMO complex[25] is shown in Figure 2 with the corresponding STFT analysis in Figure 3. Sweeping the center of the window function t_c yields information about the changes in the frequency distribution with advancing time in the exciton dynamics. In Figure 3, the initially dominant electronic coherent frequency $\hbar\omega_{15}$ is indicated by the arrow on the left side. At later times, dephasing reduces the influence of the electronic coherence while the interaction with the strongly coupled vibrational modes increases. Around $t_{\mathrm{c}} = 0.7$ ps, a "gap" can be seen where the electronic frequency is absent but shortly afterward re-emerges. From 1 to 3.5 ps a wobbling motion of the dominant contribution is seen, which is caused by the vibronic frequencies marked by arrows on the right-hand side. During the time evolution, energy is shared among different vibrational modes close in resonance with the exciton frequency $\hbar\omega_{15}$. Which vibrations are activated changes with time. For example, the vibration at $\Omega = 380$ cm^{-1} is present around 2.2 ps but

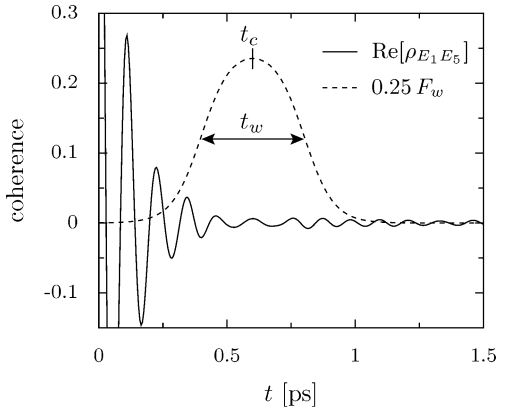

Figure 2. Time evolution of the coherence $\rho_{E_1E_5}(t)$ for the spectral density $J_{11\mathrm{peaks}}$ at $T = 150$ K. The dashed line shows a typical window function ($t_{\mathrm{c}} = 0.6$ ps, $t_{\mathrm{w}} = 0.4$ ps, $\beta = 7$).

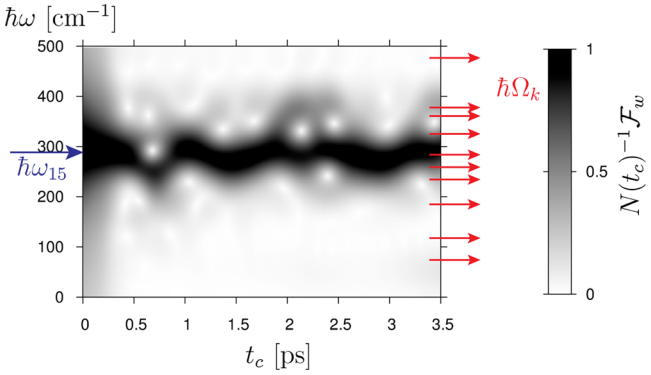

Figure 3. STFT analysis ($t_{\mathrm{w}} = 0.4$ ps, $\beta = 7$) of the coherence $\rho_{E_1E_5}$ of Figure 2. The arrow on the left marks the frequency of the electronic energy difference $E_1 - E_5$, and the arrows on the right indicate the centers of vibrational peaks of $J_{11\mathrm{peaks}}$, Figure 1.

absent around 3 ps. The features revealed in the STFT reflect two different mechanisms in the energy transfer. Electronic coherence signifies delocalized wavelike energy transfer which helps to overcome energy barriers and facilitates fast energy transfer to specific target states. On the other hand, the signatures of strongly coupled vibrational modes mark reversible energy exchange between the exciton system and the protein environment.[31]

COHERENCES IN 2D SPECTRA

The decay of peak amplitude oscillations in two-dimensional spectra has been used to extract coherence lifetimes.[5] In the following, we identify two processes which reduce the signature of electronic coherence in two-dimensional spectra compared to transport calculations. To elucidate and quantify the interplay between electronic and vibronic degrees of freedom, we discuss the physical processes mapped by 2D echo spectra within a model trimer consisting of sites 1−3 of the FMO complex[24]

$$\mathcal{H}_{\mathrm{ex}} = \begin{pmatrix} 410 & -87.7 & 5.5 \\ -87.7 & 530 & 30.8 \\ 5.5 & 30.8 & 210 \end{pmatrix} \mathrm{cm}^{-1} \tag{3}$$

As for the FMO complex,[25] we describe the energy transfer within a Frenkel exciton model[32] linearly coupled to

dx.doi.org/10.1021/jp405421d | J. Phys. Chem. B 2013, 117, 9380−9385

independent baths at each site. The spectral density is parametrized by a superposition of shifted Drude−Lorentz peaks

$$J(\omega) = \sum_{k=1}^{M} \left[\frac{\nu_k \lambda_k \omega}{\nu_k^2 + (\omega + \Omega_k)^2} + \frac{\nu_k \lambda_k \omega}{\nu_k^2 + (\omega - \Omega_k)^2} \right] \tag{4}$$

The spectral density $J_{5\text{peaks}}$ (Figure 4) for the model trimer fulfills the criteria for long-lived electronic coherences because

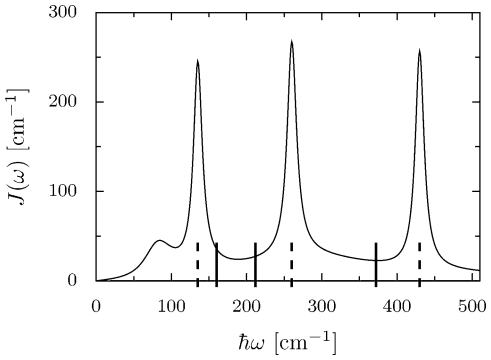

Figure 4. Five-peak model spectral density $J_{5\text{peaks}}$ with a suppressed slope at zero frequency and three strongly coupled underdamped vibrational modes. The vibrational frequencies (dashed line) are close in resonance with the difference of the exciton energies $E_i - E_j$ (solid line) of the exciton system (eq 3). Parameters for eq 4: $\lambda_k \in \{11,9,12,7,4\}$ cm^{-1}; $\nu_k^{-1} \in \{230,50,750,700,750\}$ fs; and $\hbar\Omega_k \in \{80,260,135,260,430\}$ cm^{-1}.

of its small initial slope and subsequent larger coupling. To study the role of specific vibrational modes, $J_{5\text{peaks}}$ adds three vibrational modes centered at frequencies $\hbar\Omega_1 = 135$ cm^{-1}, $\hbar\Omega_2 = 260$ cm^{-1}, and $\hbar\Omega_3 = 430$ cm^{-1}, which puts them close to resonance with the differences in exciton eigenenergies. The total 2D echo rephasing signal is composed of three Liouville pathways[33,34] reflecting stimulated emission (SE), ground-state bleaching (GB), and excited-state absorption (ESA), where the laser pulses create two excitons in the system. Formally, we calculate the Fourier transform of the third-order response function $S_{\text{RP}}(t_3,T_{\text{delay}},t_1)$[33,34] in the impulsive limit of the electric field envelope $\mathcal{E}_i(t)=\mathcal{E}_i\delta(t - t_i)\ \exp(i\omega t - ik_i r)$ which allows one to introduce a time ordering of the dipole operators for excitations and de-excitations in the response function. With the rotating wave approximation and the rephasing condition of the light direction, the three terms represented by the Liouville pathways shown in Figure 5 contribute to the signal:[35]

$$I_{\text{RP}}(\omega_1, T_d, \omega_3) = \int_0^\infty \int_0^\infty dt_1\, dt_3\, \exp(i\omega_3 t_3 - i\omega_1 t_1)$$
$$[S_{\text{RP}}^{\text{GB}}(t_3, T_d, t_1) + S_{\text{RP}}^{\text{SE}}(t_3, T_d, t_1) + S_{\text{RP}}^{\text{ESA}}(t_3, T_d, t_1)] \tag{5}$$

We include the rotational average over random orientations by sampling 20 distinct laser polarization vectors aligned along the vertices of a dodecahedron and represent the light pulses by actions of the time-ordered dipole operators.[36] We assume equal dipole strength of the three pigments and dipole orientations along the nitrogen atoms $N_B - N_D$.[37] The propagation is performed with the graphics processing units−hierarchical equations of motion (GPU−HEOM) method.[16,38] For the theoretical calculation of 2D spectra within the Frenkel exciton model, we neglect interactions of two excitons

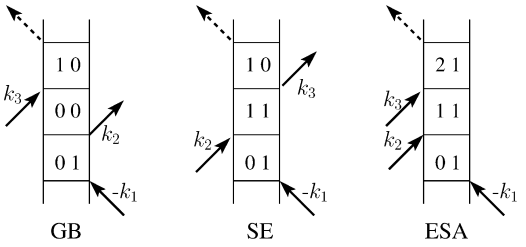

Figure 5. Time-ordering of pulses for the three rephasing contributions to the 2D echo spectra labeled ground-state bleaching (GB), stimulated emission (SE), and excited-state absorption (ESA). The population of the density matrix is denoted by the numbers, and the emitted signal (dashed arrow) points toward $k_S = -k_1 + k_2 + k_3$.

simultaneously propagating in the system and correlations between the vibronic baths at different sites. In addition, we assume an identical form of $J(\omega)$ at each site and do not include static disorder. Disorder mainly elongates the diagonal peaks in the 2D spectra, while cross-peak oscillations are damped to some extent but still undergo coherent oscillations.[25] In an experimental setup all three pathways are tied together and cannot be analyzed separately, while the theoretical calculations allows us to study the individual contributions. Typically, the SE and ESA pathways interfere destructively and lead to a diminished amplitude of the coherent signal in the total spectrum. The cancellation of coherent amplitudes in 2D spectra enhances the influence of strongly coupled vibrations on the cross-peak oscillations. In particular, the ground-state vibrations monitored by the GB get amplified in weight in the 2D echo spectra. Our finding, that ground-state vibrations affect the cross-peak dynamics, is in agreement with Tiwari et al.[39] who investigate the effect of a single vibrational mode in resonance with a model dimer. Different conditions govern transport and 2D echo spectra, where several pulses hit the sample. For instance, the ground-state bleaching and excited-state absorption induced by the 2D echo setup are not relevant for the energy transfer process. Thus, the apparent diminishing of coherences in 2D spectra does not imply unimportance of coherence in the excitonic transfer. The cancellation effects are prominently visible in Figure 6, which displays the oscillatory component of the lower-diagonal cross-peak dynamics of CP(12), CP(13), and CP(23) of the rephasing signal as a function of delay time T_{delay}. The amplitude of CP(ik) is determined by integrating the real part of the rephasing 2D spectra (all three rephasing pathways) over a small rectangle ($\Delta E = 36$ cm^{-1}) in the 2D energy grid. The center of the rectangular area is located at $\omega_i = E_i + \lambda/4.5$ and $\omega_k = E_k + \lambda/4.5$, where E_i and E_k denote the exciton eigenenergies of eq 3. The shift $\lambda/4.5$ takes into account the stokes shift and ensures that the amplitude is averaged around the maximum of the peaks. The nonoscillatory background is fitted by $f(t) = a + be^{-ct} + dt+d_2t^2$ and is subtracted from the total signal. The three cross-peaks show different behaviors. In the upper panel of Figure 6, CP(12) oscillates dominantly with a single frequency that matches the vibrational mode $\hbar\Omega_1$. The 2D spectra thus apparently shows that there is almost no remaining contribution of electronic coherence between exciton states $|E_1\rangle$ and $|E_2\rangle$. This finding is in contradiction to simulations of the coherence $\rho_{E_1E_2}(t)$ that predict long-lasting electronic coherence up to 1 ps. Studying the dynamics of the SE and ESA pathways of CP(12) separately recovers the long-lasting electronic coherence. But in the case of CP(12), the amplitudes

dx.doi.org/10.1021/jp405421d | J. Phys. Chem. B 2013, 117, 9380−9385

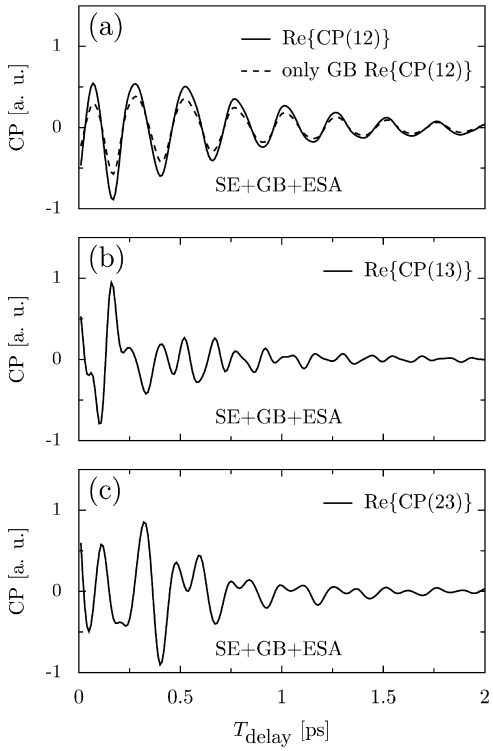

Figure 6. Oscillatory component of the real part of the cross-peak dynamics of the total rephasing 2D echo signal for eq 3 and J_{5peaks} as a function of delay time T_{delay}. The temperature is set to T = 150 K.

of the coherent oscillations of the SE and ESA pathway are nearly identical and the destructive interference of these pathways cancels the contribution of electronic coherence in the total signal. The remaining oscillatory component of the total signal reflects the ground-state vibrations of the GB pathway shown as a dashed line in Figure 6a, and the signal of electronic coherence is masked by the vibrational mode $\hbar\Omega_1$. The cross-peaks CP(13) and CP(23) (Figure 6b,c) show a more complex dynamics, which is best analyzed using the STFT methodology for the case of CP(23) in Figure 7. Multiple frequencies originating from electronic coherence and vibronic modes superpose each other and form rich structures in the beating pattern. The STFT frequency analysis for the sum of ESA and SE pathways is depicted in Figure 7a. In agreement with the STFT analysis of the coherence Re$[\rho_{E_2E_3}]$ shown in Figure 8, we observe a transition around T_{delay} = 0.7 ps from initially electronic coherence with frequency $\hbar\Omega_{23}$ = 212 cm^{-1} to vibrational frequencies $\hbar\Omega_k$ at later times. The strongest coupling to the exciton dynamics stems from the vibrational modes $\hbar\Omega_1$ and $\hbar\Omega_2$ that are close in resonance with the electronic frequency $\hbar\omega_{23}$. For the GB pathway (Figure 7b), the exciton system remains in the electronic ground state during T_{delay} and no electronic frequencies show up in the cross-peak dynamics. In the total signal (Figure 7c), the GB vibrational modes leave their trace and diminish the relative weight of the electronic coherences.

CONCLUSION

The STFT provides a tool to determine the physical mechanisms behind oscillatory signals for progressing delay time. We find that determination of electronic coherence lifetimes from the experimentally observed total signal in the

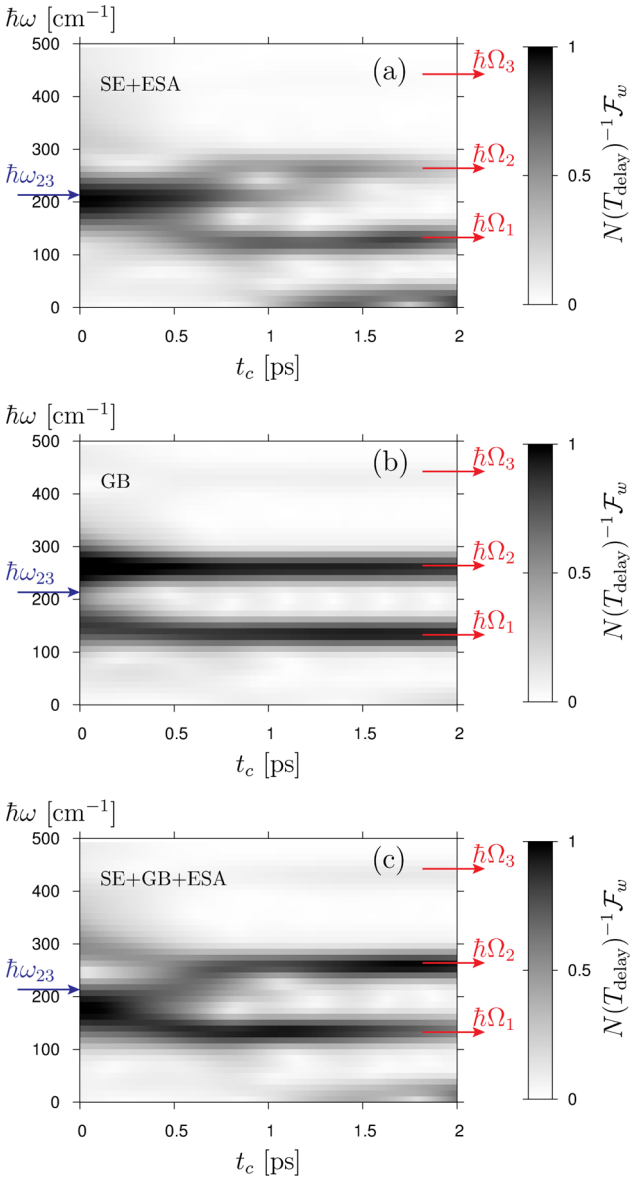

Figure 7. STFT analysis (t_w = 0.7 ps, β = 7) of the cross-peak dynamics CP(23) of the rephasing 2D echo signal at T = 150 K. Shown are results for (a) the sum of the SE and ESA pathways, (b) the contribution of the GB pathway, and (c) the total signal including all three pathways. The left arrow marks the frequency of electronic coherence $\hbar\omega_{23}$, and the right arrows mark the frequencies of the strongly coupled vibrational modes $\hbar\Omega_k$.

2D echo spectra is difficult and can underestimate the lifetime of electronic coherences. For varying delay times the STFT shows multiple frequencies and a mix of vibronic and electronic contributions. Similar observations are reported for experimentally recorded 2D spectra.[3,6,29,30] We further found examples of a reemergent amplitude in the oscillatory component at a later time in CP(23), where the amplitude at T_{delay} = 0.35 ps is larger than that seen at T_{delay} = 0.2 ps. Interestingly, such reemerging amplitudes are also observed for the FMO complex.[29,30]

The pollution of the 2D signal by ground-state vibrations and two-exciton states is not directly relevant for assessing the role of coherences in excitonic energy transfer, where these two pathways are absent. This also has implications for identifying vibronic spectral densities supporting efficient transport. We

dx.doi.org/10.1021/jp405421d | J. Phys. Chem. B 2013, 117, 9380−9385

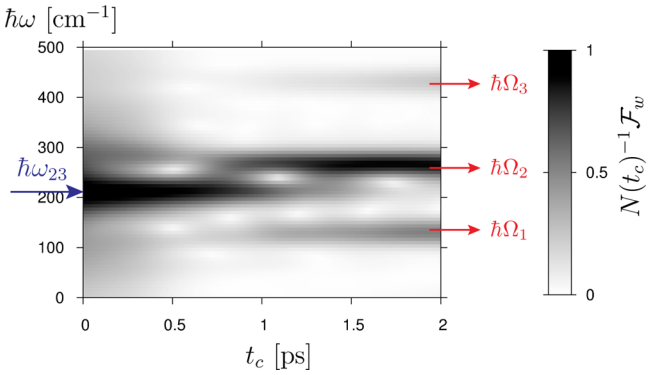

Figure 8. STFT analysis (t_w = 0.7 ps, β = 7) of the coherence Re[$\rho_{E_2E_3}$] at T = 150 K displaying behavior similar to that of the SE + ESA pathway of the 2D spectra shown in Figure 7a.

find a good correspondence between coherence lifetimes of the stimulated emission pathway (SE) of cross-peak CP(ij) and the corresponding coherence $\rho_{E_iE_j}$. For certain cross-peaks, the ground-state vibrations dominate and the 2D echo spectra are not able to determine the electronic coherence lifetime. In this case an additional analysis, such as the proposed witness of electronic coherence[40] based on broadband pump−probe measurements or quantum process tomography,[41,42] is required to reveal the hidden information.

AUTHOR INFORMATION

Corresponding Author

*E-mail: tobias.kramer@physik.hu-berlin.de.

Notes

The authors declare no competing financial interest.

ACKNOWLEDGMENTS

A.A.-G. and C.K. are supported by DARPA grants N66001-10-1-4063 and N66001-10-1-4059, and T.K. is supported by a Heisenberg fellowship of the DFG (KR 2889/5). A.A.-G. thanks the Corning foundation for their generous support.

REFERENCES

(1) Engel, G. S.; Calhoun, T. R.; Read, E. L.; Ahn, T.-K.; Mancal, T.; Cheng, Y.-C.; Blankenship, R. E.; Fleming, G. R. Evidence For Wavelike Energy Transfer Through Quantum Coherence in Photosynthetic Systems. *Nature* **2007**, *446*, 782−786.

(2) Lee, H.; Cheng, Y.-C.; Fleming, G. R. Coherence Dynamics in Photosynthesis: Protein Protection of Excitonic Coherence. *Science* **2007**, *316*, 1462−1465.

(3) Collini, E.; Wong, C. Y.; Wilk, K. E.; Curmi, P. M. G.; Brumer, P.; Scholes, G. D. Coherently Wired Light-Harvesting in Photosynthetic Marine Algae at Ambient Temperature. *Nature* **2010**, *463*, 644−647.

(4) Calhoun, T. R.; Ginsberg, N. S.; Schlau-Cohen, G. S.; Cheng, Y.-C.; Ballottari, M.; Bassi, R.; Fleming, G. R. Quantum Coherence Enabled Determination of the Energy Landscape in Light-Harvesting Complex II. *J. Phys. Chem. B* **2009**, *113*, 16291−16295.

(5) Panitchayangkoon, G.; Hayes, D.; Fransted, K. A.; Caram, J. R.; Harel, E.; Wen, J.; Blankenship, R. E.; Engel, G. S. Long-Lived Quantum Coherence in Photosynthetic Complexes at Physiological Temperature. *Proc. Natl. Acad. Sci. U.S.A.* **2010**, *107*, 12766−12770.

(6) Turner, D. B.; Dinshaw, R.; Lee, K.-K.; Belsley, M. S.; Wilk, K. E.; Curmi, P. M. G.; Scholes, G. D. Quantitative Investigations of Quantum Coherence for a Light-Harvesting Protein at Conditions Simulating Photosynthesis. *Phys. Chem. Chem. Phys.* **2012**, *14*, 4857−4874.

(7) Amerongen, H. V.; Valkunas, L.; van Grondelle, R. *Photosynthetic Excitons*; World Scientific: Singapore, 2000.

(8) Blankenship, R. E. *Molecular Mechanisms of Photosynthesis*; Blackwell Science: London, 2002.

(9) Frigaard, N.-U.; Bryant, D. A. Seeing Green Bacteria in a New Light: Genomics-Enabled Studies of the Photosynthetic Apparatus in Green Sulfur Bacteria and Filamentous Anoxygenic Phototrophic Bacteria. *Arch. Microbiol.* **2004**, *182*, 265−276.

(10) Mohseni, M.; Rebentrost, P.; Lloyd, S.; Aspuru-Guzik, A. Environment-Assisted Quantum Walks in Photosynthetic Energy Transfer. *J. Chem. Phys.* **2008**, *129*, 174106.

(11) Rebentrost, P.; Mohseni, M.; Kassal, I.; Lloyd, S.; Aspuru-Guzik, A. Environment-Assisted Quantum Transport. *New J. Phys.* **2009**, *11*, 033003.

(12) Plenio, M. B.; Huelga, S. F. Dephasing-Assisted Transport: Quantum Networks and Biomolecules. *New. J. Phys.* **2008**, *10*, 113019.

(13) Caruso, F.; Chin, A. W.; Datta, A.; Huelga, S. F.; Plenio, M. B. Highly Efficient Energy Excitation Transfer in Light-Harvesting Complexes: The Fundamental Role of Noise-Assisted Transport. *J. Chem. Phys.* **2009**, *131*, 105106.

(14) Wu, J.; Liu, F.; Shen, Y.; Cao, J.; Silbey, R. J. Efficient Energy Transfer in Light-Harvesting Systems, I: Optimal Temperature, Reorganization Energy, and Spatial-Temporal Correlations. *New J. Phys.* **2010**, *12*, 105012.

(15) Mohseni, M.; Shabani, A.; Lloyd, S.; Rabitz, H. Optimal and Robust Energy Transport in Light-Harvesting Complexes: (II) A Quantum Interplay of Multichromophoric Geometries and Environmental Interactions. 2011, arXiv:1104.4812v1. arXiv.org.

(16) Kreisbeck, C.; Kramer, T.; Rodríguez, M.; Hein, B. High-Performance Solution of Hierarchical Equations of Motion for Studying Energy Transfer in Light-Harvesting Complexes. *J. Chem. Theory Comput.* **2011**, *7*, 2166−2174.

(17) Cho, M.; Vaswani, H. M.; Brixner, T.; Stenger, J.; Fleming, G. R. Exciton Analysis in 2D Electronic Spectroscopy. *J. Phys. Chem. B* **2005**, *109*, 10542−10556.

(18) Brixner, T.; Stenger, J.; Vaswani, H. M.; Cho, M.; Blankenship, R. E.; Fleming, G. R. Two-Dimensional Spectroscopy of Electronic Couplings in Photosynthesis. *Nature* **2005**, *434*, 625−628.

(19) Christensson, N.; Kauffmann, H. F.; Pullerits, T.; Mancal, T. Origin of Long-Lived Coherences in Light-Harvesting Complexes. *J. Phys. Chem. B* **2012**, *116*, 7449−7454.

(20) Chin, A.; Prior, J.; Rosenbach, R.; Caycedo-Soler, F.; Huelga, S.; Plenio, M. The Role of Non-equilibrium Vibrational Structures in Electronic Coherence and Recoherence in Pigment−Protein Complexes. *Nat. Phys.* **2013**, *9*, 113−118.

(21) Kolli, A.; O'Reilly, E. J.; Scholes, G. D.; Olaya-Castro, A. The Fundamental Role of Quantized Vibrations in Coherent Light Harvesting by Cryptophyte Algae. *J. Chem. Phys.* **2012**, *137*, 174109.

(22) Chenu, A.; Christensson, N.; Kauffmann, H. F.; Mančal, T. Enhancement of Vibronic and Ground-State Vibrational Coherences in 2D Spectra of Photosynthetic Complexes. *Sci. Rep.* **2013**, *3*, 2029.

(23) Wendling, M.; Pullerits, T.; Przyjalgowski, M. A.; Vulto, S. I. E.; Aartsma, T. J.; van Grondelle, R.; van Amerongen, H. Electron-Vibrational Coupling in the Fenna−Matthews−Olson Complex of *Prosthecochloris aestuarii* Determined by Temperature-Dependent Absorption and Fluorescence Line-Narrowing Measurements. *J. Phys. Chem. B* **2000**, *104*, 5825−5831.

(24) Adolphs, J.; Renger, T. How Proteins Trigger Excitation Energy Transfer in the FMO Complex of Green Sulfur Bacteria. *Biophys. J.* **2006**, *91*, 2778−2797.

(25) Kreisbeck, C.; Kramer, T. Long-Lived Electronic Coherence in Dissipative Exciton Dynamics of Light-Harvesting Complexes. *J. Phys. Chem. Lett.* **2012**, *3*, 2828−2833.

(26) Shim, S.; Rebentrost, P.; Valleau, S.; Aspuru-Guzik, A. Atomistic Study of the Long-Lived Quantum Coherences in the Fenna−Matthews−Olson Complex. *Biophys. J.* **2012**, *102*, 649−660.

(27) Renger, T.; Klinger, A.; Steinecker, F.; Schmidt am Busch, M.; Numata, J.; Müh, F. Normal Mode Analysis of the Spectral Density of the Fenna−Matthews−Olson Light-Harvesting Protein: How the

Protein Dissipates the Excess Energy of Excitons. *J. Phys. Chem. B* **2012**, *116*, 14565−14580.
(28) Aghtar, M.; Strümpfer, J.; Olbrich, C.; Schulten, K.; Kleinekathöfer, U. The FMO Complex in a Glycerol−Water Mixture. *J. Phys. Chem. B* **2013**, *117*, 7157−7163.
(29) Hayes, D.; Wen, J.; Panitchayangkoon, G.; Blankenship, R. E.; Engel, G. S. Robustness of Electronic Coherence in the Fenna−Matthews−Olson Complex to Vibronic and Structural Modifications. *Faraday Discuss.* **2011**, *150*, 459−469.
(30) Panitchayangkoon, G.; Voronine, D. V.; Abramavicius, D.; Caram, J. R.; Lewis, N. H. C.; Mukamel, S.; Engel, G. S. Direct Evidence of Quantum Transport in Photosynthetic Light-Harvesting Complexes. *Proc. Natl. Acad. Sci. U.S.A.* **2011**, *108*, 20908−20912.
(31) Rebentrost, P.; Aspuru-Guzik, A. Exciton−Phonon Information Flow in the Energy Transfer Process of Photosynthetic Complexes. *J. Chem. Phys.* **2011**, *134*, 101103.
(32) May, V.; Kühn, O. *Charge and Energy Transfer Dynamics in Molecular Systems*; Wiley-VCH: Weinheim, Germany, 2004.
(33) Mukamel, S. *Principles of Nonlinear Optical Spectroscopy*; Oxford University Press: New York, 1999.
(34) Cho, M. *Two-Dimensional Optical Spectroscopy*; CRC Press: Boca Raton, 2009.
(35) Hamm, P. Principles of Nonlinear Optical Spectroscopy: A Practical Approach. 2005; http://www.mitr.p.lodz.pl/evu/lectures/Hamm.pdf
(36) Hein, B.; Kreisbeck, C.; Kramer, T.; Rodríguez, M. Modelling of Oscillations in Two-Dimensional Echo-Spectra of the Fenna−Matthews−Olson Complex. *New J. Phys.* **2012**, *14*, 023018.
(37) Adolphs, J.; Müh, F.; Madjet, M. E.-A.; Renger, T. Calculation of Pigment Transition Energies in the FMO Protein. *Photosynth. Res.* **2008**, *95*, 197−209.
(38) Kreisbeck, C.; Kramer, T. *Exciton Dynamics Lab for Light-Harvesting Complexes (GPU-HEOM)*. 2013; doi: 10.4231/D3RB6W248 online at http://nanohub.org/resources/16106.
(39) Tiwari, V.; Peters, W. K.; Jonas, D. M. Electronic Resonance with Anticorrelated Pigment Vibrations Drives Photosynthetic Energy Transfer Outside the Adiabatic Framework. *Proc. Natl. Acad. Sci. U.S.A.* **2012**, *110*, 1203−1208.
(40) Yuen-Zhou, J.; Krich, J. J.; Aspuru-Guzik, A. A Witness for Coherent Electronic vs Vibronic-only Oscillations in Ultrafast Spectroscopy. *J. Chem. Phys.* **2012**, *136*, 234501.
(41) Yuen-Zhou, J.; Aspuru-Guzik, A. Quantum Process Tomography of Excitonic Dimers from Two-Dimensional Electronic Spectroscopy. I. General Theory and Application to Homodimers. *J. Chem. Phys.* **2011**, *134*, 134505.
(42) Yuen-Zhou, J.; Krich, J. J.; Mohseni, M.; Aspuru-Guzik, A. Quantum State and Process Tomography of Energy Transfer Systems via Ultrafast Spectroscopy. *Proc. Natl. Acad. Sci. U.S.A.* **2011**, *108*, 17615−17620.